

METALLIC SURFACE RECONSTRUCTION DRIVEN BY FRUSTRATED ANTIFERROMAGNETISM

J. P. Rodriguez* and Emilio Artacho

*Departamento de Física de la Materia Condensada, C-III, and Instituto Nicolás Cabrera,
Universidad Autónoma de Madrid, Cantoblanco, 28049 Madrid, Spain.*

Abstract

A magnetic origin for the honeycomb reconstruction of metallic surfaces with three-fold symmetry like Pb/Ge (111) is proposed. Assuming that the groundstate is an antiferromagnet insulator over the triangular lattice of adatom sites (Pb), we demonstrate that the former is simultaneously unstable to canting and to a structural distortion if the surface is soft enough. We therefore predict a net magnetization over the reconstructed surface at sufficiently low temperature.

PACS Indices: 75.30.Pd, 73.20.At, 79.60.Dp

* Permanent address: Dept. of Physics and Astronomy, California State University, Los Angeles, CA 90032, USA.

The (111) surface of Ge covered with $\frac{1}{3}$ of a monolayer of Pb (or Sn) adatoms displays a striking reconstruction upon cooling.¹⁻³ At room temperature the surface is metallic, with the adatoms forming a triangular lattice. However, at low temperatures, $T < T_* \cong 250$ K, a honeycomb relief forms over the triangular adatom structure. This transition from a $\sqrt{3} \times \sqrt{3}$ surface structure at ambient temperature to a reconstructed 3×3 surface at low temperature is observed directly via scanning electron microscopy (STM) and by low-energy electron diffraction (LEED) techniques. The reconstruction is also reflected in the electronic structure of the surface. In particular, both angle-resolved photo emission spectra (ARPES) and electron energy loss spectra (EELS) find that a pseudogap opens at the Fermi surface of the surface conduction band at temperatures below T_* .^{4,5} Such measurements suggest that the reconstructed surface has an *insulating* groundstate.

It was originally proposed that the 3×3 surface reconstruction is due to a charge-density wave (CDW) instability within the metallic $\sqrt{3} \times \sqrt{3}$ surface.¹ The absence of good nesting properties of the Fermi surface at room temperature²⁻⁵ indicates, however, that this is unlikely. To account for the phenomenon that remains, we propose instead that the reconstructed surface is an antiferromagnetic Mott insulator^{6,7} composed of localized spin-1/2 moments associated with the dangling chemical bond left at each adatom site. Both the narrowness of the surface conduction band^{4,8} and the presence of the low-temperature pseudo-gap feature^{1,5} make this idea plausible. In the limit of large on-site repulsion, we are then left with an antiferromagnetic Heisenberg model description for the electronic spins that remain over the sites of the triangular lattice of adatoms. A classical analysis of this model in combination with magnetostriction phenomenology⁹ leads us to conclude that the magnetic frustration intrinsic to antiferromagnetism on a triangular lattice drives a soft enough $\sqrt{3} \times \sqrt{3}$ surface to buckle or dilate with the periodicity of a honeycomb relief. We therefore predict that the low-temperature 3×3 surface reconstruction has a structural component. The original LEED evidence for the reconstruction of the Pb/Ge (111) surface¹ as well as recent surface X-ray diffraction studies^{10,11} support this point of view. Coincident with the honeycomb distortion is a canted antiferromagnetic spin arrangement with reduced frustration (see Fig. 1). We therefore also predict a net magnetization over the reconstructed surface at low enough temperatures.

We begin the theoretical discussion at zero temperature, where a Mott insulator

state^{6,7} is assumed for the reconstructed metallic surface.¹ Specifically, suppose that a localized spin $s = \frac{1}{2}$ moment, \vec{S}_i , lies at each site, i , of the triangular lattice coincident with the Pb (or Sn) adatoms. The former represents the spin associated with the dangling chemical bond on the Pb/Ge (111) surface. The simplest description of this system is an antiferromagnetic Heisenberg model

$$H = \sum_{\langle ij \rangle} (J_{ij} \vec{S}_i \cdot \vec{S}_j + \delta J_{ij} S_i^z S_j^z) - \vec{h} \cdot \sum_i \vec{S}_i \quad (1)$$

summed over nearest-neighbor bonds $\langle ij \rangle$ on the triangular lattice. Here, $J_{ij} > 0$ denotes the exchange coupling constant over such bonds, while \vec{h} denotes the external magnetic field. Also, the parameter δ is a measure of the magnetic anisotropy along the z -axis perpendicular to the surface that originates from the spin-orbit interaction. We now take the key step in the theory by supposing that a honeycomb lattice distortion accompanies the Mott insulator state (1), and that this results in two different exchange coupling constants, J and J' , over the undistorted and distorted bonds, respectively (see Fig. 1). The buckled (dilated) lattice is achieved by raising (expanding) or lowering (contracting) the regions in the vicinity of the honeycomb (a and b sites) with respect to those regions in the vicinity of the centers (c sites) of the honeycomb. The phenomenology

$$J_{ij} = J_0 + J_1(\eta_i + \eta_j) \quad (2)$$

for the exchange coupling constant of the distorted lattice is compatible with these assignments. Here J_1 is the first order magnetostriction coefficient⁹ with respect to the scalar field η_i , which can represent either perpendicular displacements, u_z , or lateral dilations, $\partial_x u_x + \partial_y u_y$, of the (triangular lattice) surface in the vicinity of adatom i . Equations (1) and (2) represent the essential components of the theory.

We now analyze the isotropic ($\delta = 0$) antiferromagnetic model (1) in the classical limit, $s \rightarrow \infty$, in which case the spin operator \vec{S}_i reduces to a 3-vector of magnitude s . The ground state for the honeycomb arrangement of exchange coupling constants $J_{ab} = J$ and $J_{ac} = J' = J_{bc}$ indicated in Fig. 1 is a *canted* three-fold symmetric spin configuration over the three sublattices a , b , and c , of the honeycomb-distorted lattice. This canted antiferromagnet has a net magnetization

$$\vec{S} = \frac{1}{3}(\vec{S}_a + \vec{S}_b + \vec{S}_c) = \frac{1}{3}(1 - 2 \cos \theta) \vec{S}_c \quad (3)$$

aligned parallel to the sublattice magnetization, \vec{S}_c , of the c sites, where θ represents the half angle in between spins \vec{S}_a and \vec{S}_b (see Fig. 1). Since this macroscopic moment must be aligned along the external magnetic field, \vec{h} , we obtain an energy per site

$$E_M/N = s^2 J \cos(2\theta) + 2s^2 J' \cos(\pi - \theta) - E_Z |\vec{S}| \quad (4)$$

for the canted antiferromagnet, where $E_Z \propto |\vec{h}|$ denotes the Zeeman energy splitting. If we define $\Delta J = J' - J$, then the minimum energy occurs at a half angle θ_0 such that $\cos \theta_0 = [s^2 J' + \frac{1}{3}(\text{sgn } \Delta J) s E_Z] / 2s^2 J$, with energy

$$E_M/N = -s^2 J - \frac{[sJ' + \frac{1}{3}(\text{sgn } \Delta J) E_Z]^2}{2J} + \frac{1}{3}(\text{sgn } \Delta J) s E_Z, \quad (5)$$

and with net magnetization

$$\vec{S} = -\frac{1}{3} \left(\frac{\Delta J}{J} + \frac{\text{sgn } \Delta J}{3} \frac{E_Z}{sJ} \right) \vec{S}_c. \quad (6)$$

Notice that both an external surface strain [see Eq. (2) and ref. 9] and an external magnetic field increases canting, and the saturated magnetization, \vec{S} , as a result.

Above, we have shown how a honeycomb distortion of the frustrated antiferromagnet on the triangular lattice lowers the magnetic energy via magnetostriction. But is such a canted antiferromagnetic state energetically favorable with respect to the distorted lattice itself? We return to the magnetostriction phenomenology (2) to address this question. Suppose that the triangular lattice has a honeycomb distortion, with lateral dilations or perpendicular displacements $\eta_a = \eta_b$ at the honeycomb, and with lateral dilations or perpendicular displacements η_c at the centers. Macroscopic stability of the surface requires that

$$\eta_a + \eta_b + \eta_c = 0. \quad (7)$$

This fact coupled with expression (5) for the magnetic energy in the absence of magnetic field, in addition to the magnetostriction phenomenology (2), yields the new expression

$$E_M/N = -s^2 \left[\frac{3}{2} J_0 + \bar{J}_2 (\eta_a - \eta_c)^2 \right] \quad (8)$$

that is valid up to quadratic order in the displacements, where

$$\bar{J}_2 = \frac{1}{2} \frac{J_1^2}{J_0} \quad (9)$$

is the effective second order magnetostriction coefficient of the distorted lattice. Therefore, if the bare energy for a lattice distortion has the effective form $E_L = \frac{1}{2}\bar{k}_0 \sum_{\langle ij \rangle} (\eta_i - \eta_j)^2$, then the system as a whole, $E = E_L + E_M$, is unstable to a honeycomb-type buckling or dilation for soft surfaces such that

$$s^2 \bar{J}_2 > 2\bar{k}_0. \quad (10)$$

Here, \bar{k}_0 denotes the relevant effective spring constant for the case of a buckling distortion. We therefore observe that the frustrated antiferromagnetism that exists on the triangular lattice of spins *drives* the honeycomb distortion in order to improve magnetic energy on the soft surface (10). Last, Eqs. (4)-(6) indicate that this effect is only *enhanced* by the application of an external magnetic field!

Yet what effect do the quantum fluctuations that are connected with the localized spin-1/2 moments have on this honeycomb-type lattice instability? It is known that frustration generally decreases the spin stiffness of a spin-1/2 antiferromagnet.¹² In our notation, the spin stiffness is essentially the prefactor s^2 in expression (8) for the magnetic energy. This means that quantum corrections renormalize down s^2 to a function s_R^2 of frustration that has a minimum at $J = J'$, in which case the frustration is at a maximum. Hence, quantum corrections can only *enhance* the honeycomb lattice instability (10) driven by frustration in the antiferromagnet (relative to the undistorted triangular lattice [see Eq. (8)]).

We have seen how a canted antiferromagnetic spin arrangement over the triangular lattice can induce a buckling or dilation instability with a periodicity of the honeycomb type. Strictly speaking, the effect requires long range order among the magnetic moments. A “large- N ” analysis of the continuum energy functional

$$E_M = \frac{1}{2}\rho_s \int d^2r [(\vec{\nabla} \vec{m})^2 \pm \xi_0^{-2} m_z^2] \quad (11)$$

with respect to the normalized sublattice magnetization ($|\vec{m}| = 1$) of the effective *classical* Heisenberg model (1) indicates that this is indeed the case at temperatures below a critical temperature,¹³ $k_B T_c \cong 2\pi\rho_s / \ln|\delta|^{-1}$. Here, $\rho_s = s_R^2 J$ denotes the relevant spin stiffness,¹³ while $\delta' = a'^2 / \xi_0^2$ is a measure of the magnetic anisotropy along the z -axis perpendicular to the 3×3 surface with lattice constant a' . The anisotropy δ' is assumed to be small. A net macroscopic moment is then predicted to exist over the (3×3) surface at such low temperatures, $T < T_c$. At high temperatures, $T > T_c$, the magnetic correlation

length, $\xi_M(T)$, is finite. Clearly, the honeycomb lattice instability (10) cannot occur if the magnetic correlation length is short compared to the lattice constant. This suggests the (implicit) definition $\xi_M(T_*) = a'$ for the paramagnetic cross-over temperature, $k_B T_* \sim 2\pi\rho_s$. At intermediate temperatures $T_c < T < T_*$, we expect to have fluctuating domains of ferrimagnetic order, each with dimensions of order $\xi_M(T)$. A *short-range* honeycomb lattice instability (10) is then possible. In such case, we expect a diffuse Bragg diffraction pattern corresponding to the 3×3 surface.

In the regime of high temperatures, $T > T_* \sim J/k_B$, our simple model [Eqs. (1) and (2)] thus predicts a paramagnetic insulator state over an *undistorted* triangular lattice. This prediction, clashes, however, with experimental evidence for the existence of a metallic surface at ambient temperatures above the reconstruction temperature, T_c . The electronic charge fluctuations that are suppressed in the Heisenberg model (1) must therefore be included. We resort to the nearest-neighbor Hubbard model

$$H = - \sum_{\langle ij \rangle, \sigma} t_{ij} c_{i\sigma}^\dagger c_{j\sigma} + \sum_i U_i n_{i\uparrow} n_{i\downarrow} \quad (12)$$

on the triangular lattice at half filling to address this problem. Here, $c_{i\sigma}$ denotes the annihilation operator for an electron of spin σ at site i , while $n_{i\sigma}$ is the corresponding occupation number. In the limit of strong on-site repulsion, $U_i \rightarrow \infty$, we recover the antiferromagnetic insulator state (1) already discussed, with exchange coupling constants⁶

$$J_{ij} = 2t_{ij}^2 (U_i^{-1} + U_j^{-1}). \quad (13)$$

Let us consider the weak-coupling limit $U_i = 0$ instead, and suppose that a honeycomb lattice distortion is “frozen in”. The electron-phonon interaction then results in two different nearest-neighbor hopping amplitudes, $t_{ab} = t$ and $t_{ac} = t' = t_{bc}$, in between the sublattices (see Fig. 1). Assuming Bloch waves of momentum \vec{k} for the one-electron states over each sublattice, we obtain a corresponding spectrum $\varepsilon_{\vec{k}}$ that satisfies the characteristic equation

$$0 = \varepsilon_{\vec{k}}^3 - (2t'^2 + t^2) |\alpha_{\vec{k}}|^2 \varepsilon_{\vec{k}} + t'^2 t (\alpha_{\vec{k}}^3 + \alpha_{\vec{k}}^{*3}), \quad (14)$$

where the amplitude

$$\alpha_{\vec{k}} = e^{i\vec{k} \cdot \vec{a}_1} + e^{i\vec{k} \cdot \vec{a}_2} + e^{i\vec{k} \cdot \vec{a}_3} \quad (15)$$

is a sum over the (overcomplete) basis, $\vec{a}_1 = a\hat{x}$ and $\vec{a}_{2,3} = (a/2)(-\hat{x} \pm 3^{1/2}\hat{y})$, of the triangular lattice (see Fig. 1). This system has two noteworthy limits: (i) On the undistorted triangular lattice, $t = t'$, we have a single band of surface conduction electrons that disperses as

$$\varepsilon_{\vec{k}} = -t(\alpha_{\vec{k}} + \alpha_{\vec{k}}^*). \quad (16)$$

The density of states per site at the Fermi surface for the half-filled band is $N(0) \sim W^{-1}$, where $W = 9t$ gives the bandwidth. The Fermi surface itself at half filling is nearly circular and evidently shows no nesting (see Fig. 2, at $T > T_c$). (ii) In the case of an extreme honeycomb distortion, $t \ll t'$ or $t' \ll t$, we have two graphene-type bands that are separated by a small gap at the vertices ($K_{3 \times 3}$) of the Brillouin zone boundaries that correspond to the honeycomb. Within this gap lies a narrow band,

$$\varepsilon_{\vec{k}} = \bar{t}(\alpha_{\vec{k}}^3 + \alpha_{\vec{k}}^{*3})/|\alpha_{\vec{k}}|^2, \quad (17)$$

that crosses the Fermi surface at half filling, with an effective hopping amplitude $\bar{t} = \frac{1}{2}t$ and $\bar{t} = t'^2/t$ in the respective limits $t \rightarrow 0$ and $t' \rightarrow 0$. This band has a global maximum at the center of the Brillouin zone ($\Gamma_{3 \times 3}$) and a global minimum at the points $M_{3 \times 3}$ that lie in between neighboring $K_{3 \times 3}$ points. The Fermi surface at half filling for this low-temperature ($T < T_c$) band structure is displayed in Fig. 2. The combined effect of a narrow bandwidth, $\bar{W} = 8\bar{t}$, and of the ‘‘corners’’ present in the Fermi surface result in a relatively large density of states, $N(0) \gtrsim \bar{W}^{-1}$, there.

In light of these observations, we propose the following mechanism that accounts for the metallicity of the unconstructed surface. At high temperatures $T > T_c$, the electronic states at the surface are described by a half-filled nearest-neighbor Hubbard model (12) over the triangular lattice, $t = t'$, with an on-site repulsion U below the critical one, $U_c \sim W$, at the Mott transition.⁷ This is consistent with a metallic state. At low temperatures, $T < T_c$, the surface buckles or dilates ($t \neq t'$) in order to lower its magnetic energy ($J \neq J'$). In particular, the honeycomb distortion of the triangular lattice of adatoms results in a narrow band (17) that crosses the Fermi surface through the effects of the electron-phonon interaction. The presence of an insulating magnetic groundstate at zero temperature then requires that the on-site repulsion U now be *greater* than the new critical one, $U_c \sim \bar{W}$, at the Mott transition.⁷ This means, in rough terms, that the on-site repulsive energy must

lie inside the window $\bar{W} < U < W$ of parameter space. Last, the Fermi surface of the reconstructed metallic surface (see Fig. 2, at $T < T_c$) should be unstable to the formation of an SDW due to the relatively large density of states connected with the narrow low-temperature band (17).¹⁴ Since the electron-phonon interaction induces magnetostriction (2) through the identity (13), the previous strong-coupling analysis indicates that this SDW state is precisely the canted antiferromagnetic arrangement of spins depicted in Fig. 1. We then notably predict that the reconstructed surface has a net magnetization (6) at low temperatures, $T < T_c$. An analysis of the Hubbard model (12) within the mean-field approximation indicates that such a net moment causes the conduction bands (17) of the reconstructed surface to split in a manner similar to Fe.⁸

Yet how does the above proposal compare with experiment? First, the presence of an SDW gap at the Fermi surface is consistent with evidence that points towards the existence of an insulating state on the reconstructed Pb/Ge (111) surface at low temperature: e.g., STM images, EELS and surface photo-emission spectra.^{1,4} Second, the band structure characteristic of a honeycomb distortion of the triangular lattice (17) is consistent with recent ARPES studies of the reconstructed Pb/Ge (111) surface⁵ that see the gap expected by zone folding at the $M_{3 \times 3}$ points of the Brillouin zone. Even more striking is the fact that such ARPES experiments observe iron-type splitting of surface conduction electrons bands! This of course is consistent with the presence of a net magnetic moment,⁸ which we propose is due to the canted antiferromagnetic Mott insulator state shown in Fig. 1. Last, both LEED and recent X-ray diffraction studies find evidence for a periodic (3×3) structural distortion of the reconstructed Pb/Ge (111) surface that is consistent with the honeycomb distortion proposed here.^{1,10,11}

Contrary to expectations based on the width of the surface conduction electron band,² however, the 3×3 reconstruction presented by the Sn/Ge (111) surface appears at temperatures below $T_* \cong 210$ K, which is appreciably lower than that corresponding to the Pb/Ge (111) surface. And unlike the latter, the Sn/Ge (111) surface appears to remain metallic down to a temperature $T = 110$ K.^{2,3} We speculate that such discrepancies between the Pb and Sn adatoms surfaces originate from the elemental differences in the spin-orbit coupling. The relatively weak spin-orbit coupling present in the Sn adatom results in a smaller magnetic anisotropy δ [see Eqs. (1) and (11)], and thus in both a lower magnetic

rigidity, $k_B T_*$, and critical temperature, T_c .

This work was supported in part by National Science Foundation grant No. DMR-9322427 and by the Spanish grant No. DGES PB95-0202. The authors are indebted to E.G. Michel and to F. Guinea for discussions.

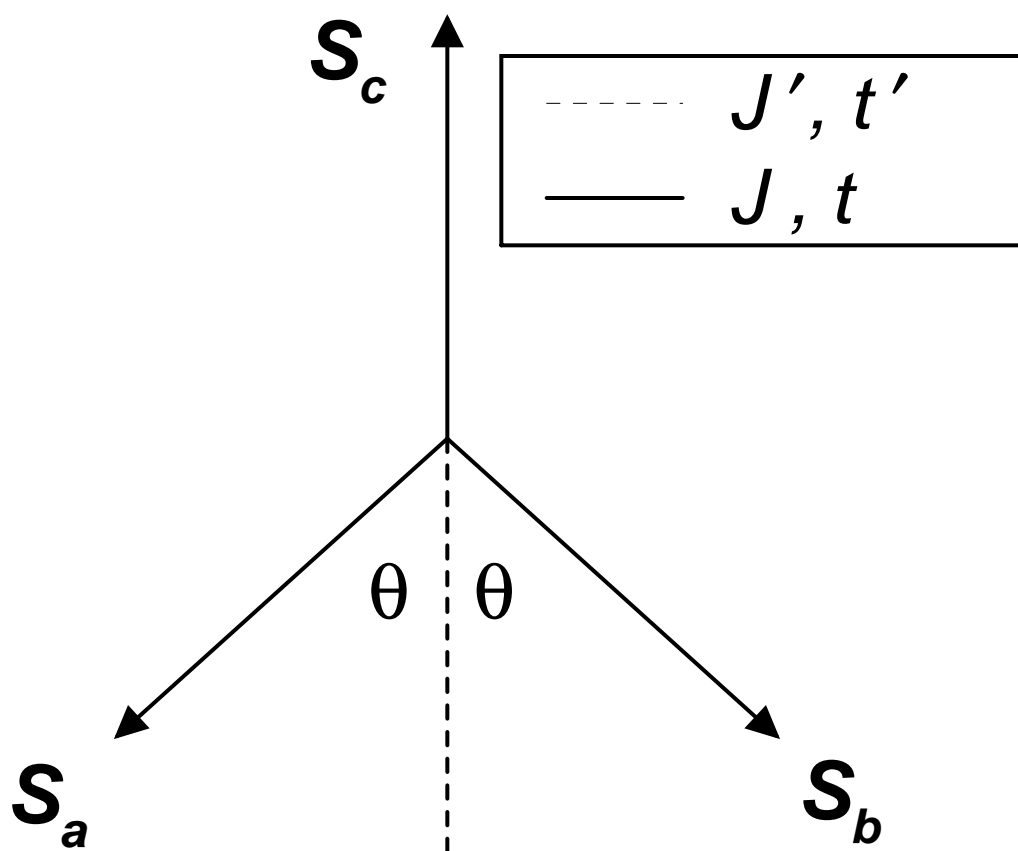
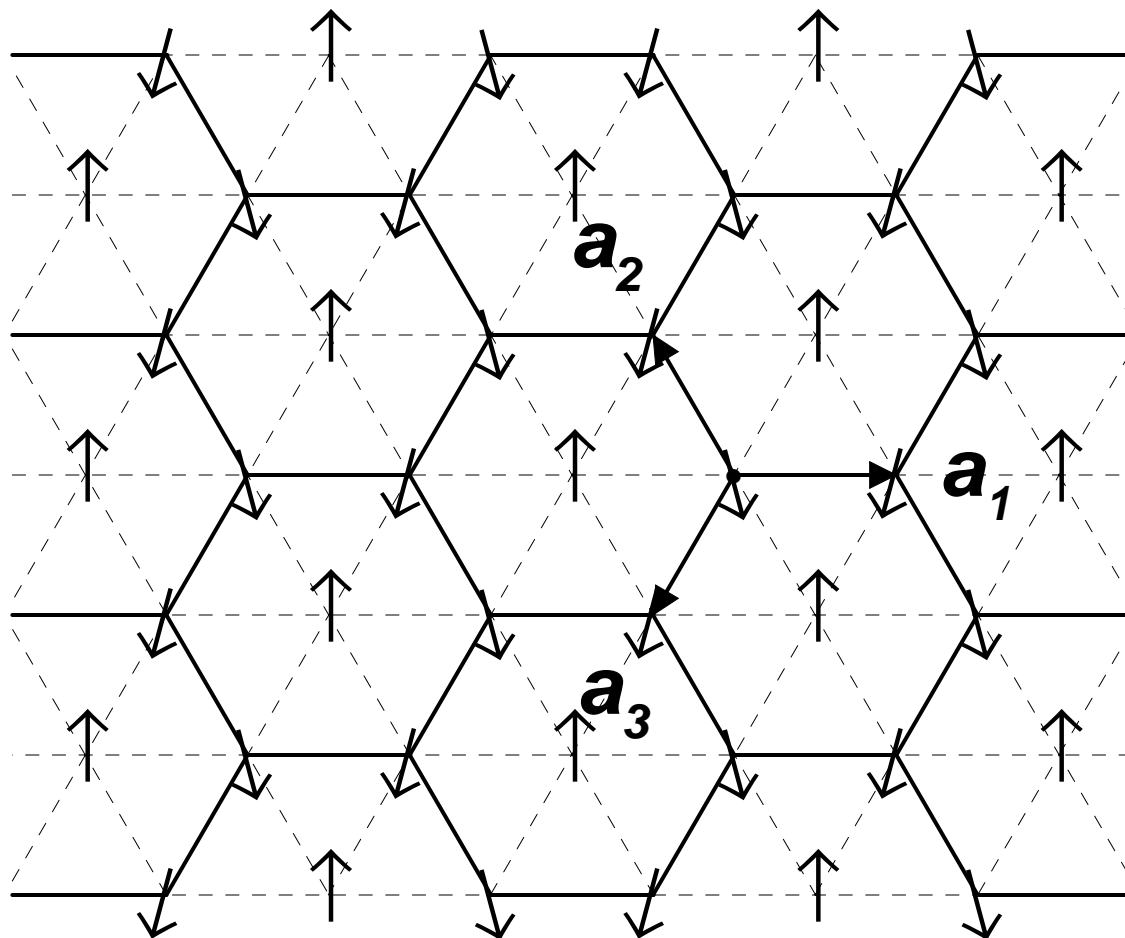
References

1. J.M. Carpinelli et al., *Nature* **381**, 398 (1996).
2. J.M. Carpinelli et al., *Phys. Rev. Lett.* **79**, 2859 (1997).
3. A. Goldoni and S. Modesti, *Phys. Rev. Lett.* **79**, 3266 (1997).
4. A. Goldoni et al., *Phys. Rev. B* **55**, 4109 (1997).
5. A. Mascaraque et al., *Phys. Rev. B* **57**, 14758 (1998); A. Mascaraque et al., *Surf. Sci.* **404**, 742 (1998).
6. P.W. Anderson, *Phys. Rev.* **115**, 2 (1959).
7. W.F. Brinkman and T.M. Rice, *Phys. Rev. B* **2**, 4302 (1970); for a review, see A. Georges et al., *Rev. Mod. Phys.* **68**, 13 (1996).
8. G. Santoro et al., *Surf. Sci.* **404**, 802 (1998); S. Scandolo et al., *Surf. Sci.* **404**, 808 (1998).
9. L.D. Landau and E.M. Lifshitz, *Electrodynamics of Continuous Media* (Addison-Wesley, Reading, 1960) chap. 5.
10. A.P. Baddorf et al., *Phys. Rev. B* **57**, 4579 (1998).
11. A. Mascaraque et al. (unpublished).
12. J. Bonča et al., *Phys. Rev. B* **50**, 3415 (1994); J.P. Rodriguez et al., *Phys. Rev. B* **51**, 3616 (1995).
13. A.M. Polyakov, *Gauge Fields and Strings* (Harwood, New York, 1987).
14. J.R. Schrieffer et al., *Phys. Rev. Lett.* **60**, 944 (1988).

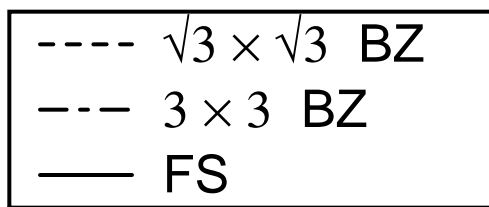
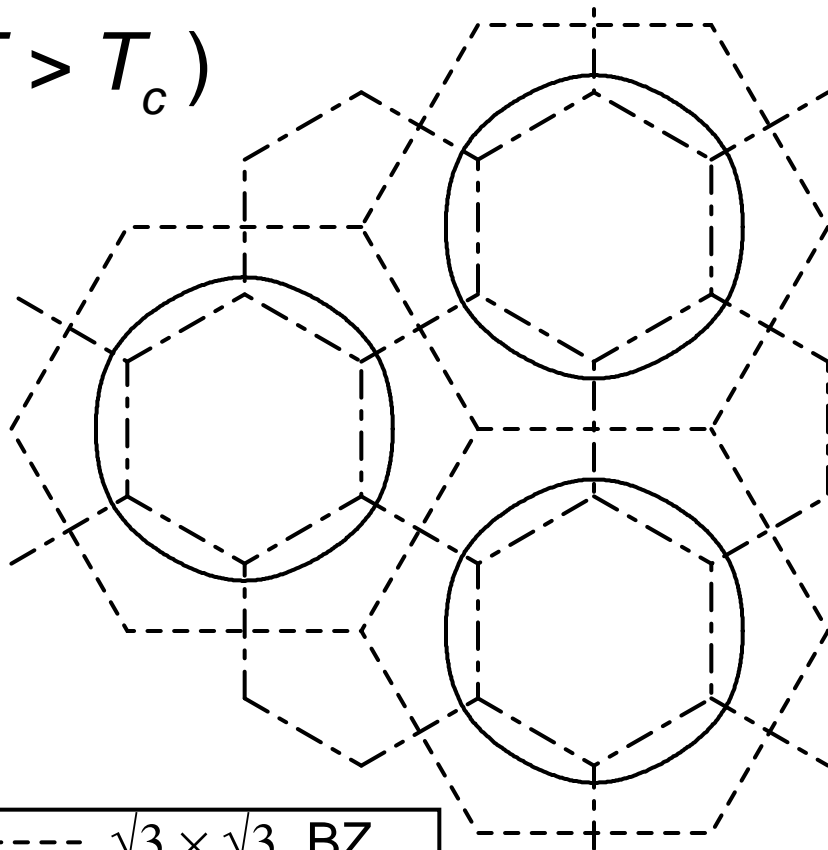
Figure Caption

Fig. 1 Shown is the canted antiferromagnetic spin arrangement over the 3×3 lattice.

Fig. 2 The Fermi surface (FS) for both the low-temperature (17) and the high-temperature (16) band structures at half filling are displayed. Also displayed are the corresponding Brillouin zone (BZ) boundaries.



$(T > T_c)$



$(T < T_c)$

